

Picosecond ultrasonic measurements of attenuation of longitudinal acoustic phonons in silicon

B. C. Daly

Physics and Astronomy Department, Vassar College, Poughkeepsie, New York 12604, USA

K. Kang, Y. Wang, and David G. Cahill

Materials Research Laboratory, Department of Materials Science and Engineering, University of Illinois, Urbana, Illinois 61801, USA

(Received 28 September 2009; published 19 November 2009)

We report ultrafast optical measurements of the attenuation of 50 and 100 GHz longitudinal acoustic-phonon pulses in Si. Picosecond acoustic measurements were made at temperatures $50 < T < 300$ K on thinned (50- μm -thick) wafers. The measured phonon lifetimes at 300 K, ≈ 5 –7 ns, are an order of magnitude less than expected based on three-phonon scattering rates derived from thermal conductivity data. We find instead that relaxational damping is the dominant mechanism in this frequency and temperature range. This attenuation sets an intrinsic limit on the quality factor of nanomechanical resonators that operate near room temperature.

DOI: [10.1103/PhysRevB.80.174112](https://doi.org/10.1103/PhysRevB.80.174112)

PACS number(s): 63.20.kg, 42.65.Re, 43.58.+z

The attenuation of high-frequency acoustic waves in dielectric or semiconductor crystals is a topic with a long history that also has a critical importance to several areas of current interest in condensed matter and materials physics. First, long-wavelength acoustic phonons with frequencies near 1 THz are expected to play an important role in nanoscale heat transport.¹ Recent work suggests that long wavelength phonons with mean free paths larger than 1 μm are responsible for a significant portion of the thermal conductivity in Si at 300 K.^{2,3} Second, the feasibility of imaging buried nanostructures using high-frequency acoustic waves will depend on attenuation levels at different temperatures and frequencies.^{4,5} Finally, high-quality factor nanomechanical resonators in the GHz frequency range^{6,7} have potential for device applications but the intrinsic attenuation mechanisms are not yet fully understood. Recent experiments on ~ 1 THz phonons in 200–300 nm suspended Si membranes suggest that acoustic phonons in confined geometries may possess lifetimes that are longer than their bulk counterparts,⁸ while measurements of 7 nm GaAs nanocavities indicate that the anharmonic contribution to the phonon lifetime is similar to bulk values.⁹

In an effort to better understand the lifetimes of subterahertz acoustic phonons in bulk crystals, we have made picosecond ultrasonic measurements of attenuation in a thin Si wafer in the temperature range $50 < T < 300$ K at 50 and 100 GHz. Attenuation of acoustic phonons in this frequency range in Si has been studied previously by Hao and Maris,¹⁰ but only at temperatures lower than 130 K. The highest frequency for which the attenuation in Si has previously been measured at room temperature is 20 GHz.¹¹ At this frequency range, the acoustic-phonon wavelength is on the order of 100 nm. This is comparable to the mean free paths of the higher frequency thermal phonons that are the dominant carriers of heat flow in insulating and semiconducting crystals.

In a crystalline semiconductor such as Si, the dominant mechanism for the decay of an ultrasonic wave is its interaction with thermal phonons.¹² The mechanism is expected to take one of two forms, depending on the frequency and temperature regimes. For ultrasonic waves at high frequencies and low temperatures such that the acoustic wave frequency satisfies $\omega \sim kT/\hbar$, the attenuation is best described

by three-phonon anharmonic decay processes as originally put forth by Landau and Rumer¹³ and later by Pomeranchuk.¹⁴ For lower frequency ultrasound the decay mechanism is expected to follow a relaxation damping theory due to Akhieser,¹⁵ where the sound waves disturb the occupation of thermal phonons whose frequencies depend on strain. The thermal phonons then collide with one another, returning the system to equilibrium as energy is removed from the sound wave. For our measurements, the ultrasound waves of interest are of a much lower frequency than the average thermal phonon frequency which places us in a regime where either or both mechanisms could conceivably contribute to the attenuation. We further subcategorize the frequency and temperature range into the regimes $\omega\tau \gg 1$ and $\omega\tau \ll 1$ where τ is the average lifetime of the thermally excited phonons in the crystal. At lower temperatures we find ourselves squarely in the $\omega\tau \ll 1$ regime, but at room temperature where optical phonon lifetimes¹⁶ in Si are ≈ 2 ps and acoustic-phonon lifetimes are ≈ 30 ps we very nearly approach $\omega\tau = 1$.

Ultrasonic attenuation in Si due to anharmonic three phonon processes, i.e., the Landau-Rumer mechanism, should have a quadratic dependence on frequency. An important paper by Herring¹⁷ demonstrated that this should be true for many types of crystals even at low temperatures and long wavelengths. His work extended the Landau and Rumer model to account for the types of phonon collisions that are allowed by the crystalline anisotropy. Herring's result is that the attenuation of a phonon should vary with frequency and temperature as $\omega^a(kT/\hbar)^{5-a}$, where $a=2$ for cubic crystals such as Si. This dependence on frequency and temperature was recently observed for 470 and 940 GHz phonons in GaN.¹⁸

In contrast, ultrasonic attenuation as described by Akhieser's relaxation damping exhibits a more complex frequency dependence. The full expression for the attenuation α using relaxation damping theory is given in Eq. 130 of Ref. 12. Two components of the attenuation mechanism are represented: (i) a phonon viscosity due to the Akhieser mechanism and (ii) thermoelastic damping caused by thermal conduction between regions of differing acoustic strain. Here we reproduce a simplified expression that is valid for all values of $\omega\tau$

in cases where the thermoelastic damping is negligible. The attenuation α is then

$$\alpha = \frac{CT}{2\rho s^3} \frac{\omega^2 \tau}{1 + \omega^2 \tau^2} (\langle \gamma^2 \rangle - \langle \gamma \rangle^2), \quad (1)$$

where C is the volumetric heat capacity, ρ is the density, s is the speed of the ultrasound wave, and γ is the Grüneisen parameter of the thermal phonons.¹² The brackets $\langle \dots \rangle$ indicate averages taken over the entire spectrum of thermally excited phonons. The attenuation should have a quadratic dependence on frequency for $\omega\tau \ll 1$ but should exhibit no frequency dependence for $\omega\tau \gg 1$. To determine whether it is valid to disregard the contribution of thermoelastic damping we used an approximate formula given by Duquesne and Perrin, see Eq. 6 of Ref. 11, and found that thermoelastic damping contributes an additional 10% to the Akhieser attenuation at 50 GHz and an additional 30% to the Akhieser attenuation at 100 GHz.

The samples were undoped Si [100] wafers that had been thinned to between 52 and 55 μm and polished on both sides. The resistivity of the Si indicated that doping levels were less than 10^{14} cm^{-3} although Si grown by the Czochralski method can have oxygen impurities as high as 10^{18} cm^{-3} . Such impurity concentrations will contribute a negligible amount of scattering to 50 and 100 GHz phonons.¹⁹ The samples were coated with Al films ranging in thickness from 10 to 25 nm that were used as transducers. A mode-locked Ti:sapphire oscillator with a repetition rate of 80 MHz was used to perform the pump-probe experiments.²⁰ Both pump and probe were focused to an 8 μm $1/e^2$ radius spot on the Al-film surface. The pump pulses (800 nm, ~ 200 fs, 0.2 nJ) from the oscillator rapidly heated the Al film, generating coherent longitudinal acoustic-phonon pulses through a thermoelastic effect.²¹ The pulses are coherent in the sense that all of the excited phonon modes have a definite phase relationship, in contrast to an incoherent pulse (a heat pulse). These phonon pulses that are transmitted from the Al into the Si are roughly single cycle in nature with a compressive strain leading a rarefying strain. The magnitude of the strain is $\sim 10^{-4}$. The spectrum of the phonon pulses depends on the thickness of the Al transducers but typically peak frequency and bandwidth will be on the order of 100 GHz. An electro-optic modulator operating at 9.8 MHz was used to modulate the pump beam and lock-in amplification was used in the detection of the reflected probe beam. The thickness of the Si was chosen so that phonon pulses completed a single round trip through the Si in a time comparable to the 12.5 ns repetition period of the oscillator. An optical delay stage with a range of 4 ns allowed detection of phonon pulses that had traveled one or two round trips through the Si.^{4,10,11}

Figure 1 shows the reflectivity changes $\Delta R(t)$ caused by the phonon pulses after one and two round trips at five temperatures ranging from 100 to 300 K. Temperature control was provided by an optical cryostat with a cold finger. The data were taken on a sample with a 20 nm Al film. $\Delta R(t)$ is directly proportional to the strain and is a convolution of the amplitude of the traveling acoustic pulse and the optical sensitivity function of the Al film.²¹ The thermal backgrounds of

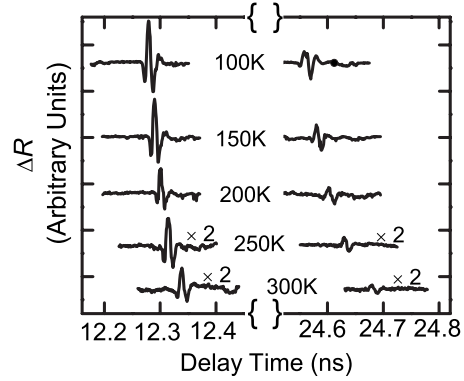


FIG. 1. $\Delta R(t)$ for a 20 nm Al-film sample. Phonon pulses are shown after one (12.3 ns) and two (24.6 ns) round trips in the Si wafer. The signals at 250 and 300 K are multiplied by a factor of two to allow visual comparison.

the data have been removed and each data set has been offset for clarity. To obtain the curves shown in Fig. 1, we accounted for the effects of the 9.8 MHz pump modulation. Since the modulation period is 102 ns, the phonon signal at 12.3 ns arrives roughly 45° out of phase with the lock-in reference signal. Thus, the in-phase V_{IN} and out-of-phase V_{OUT} outputs are related by $V_{IN} \approx V_{OUT} \approx V_{MAG} / \sqrt{2}$. For the signal at 24.6 ns, $V_{IN} \approx 0$ and $V_{OUT} \approx V_{MAG}$. We used the out-of-phase component of the lock-in signal and multiplied the 12.3 ns signal by $\sqrt{2}$ before representing it in Fig. 1 as a measure of $\Delta R(t)$.

A number of observations can be made upon inspection of Fig. 1. First, the temperature dependence of $\Delta R(t)$ is indicated by the multiplicative factors that have been placed on the figure. While the bulk of this dependence is expected to be the temperature dependence of the acoustic attenuation, some part of it may arise from changes in the sensitivity and absorption of the Al transducer. Second, the variation in arrival times as a function of temperature is indicative of the temperature dependence of the sound velocity. We find, as expected, a $\approx 0.5\%$ change in the longitudinal sound velocity

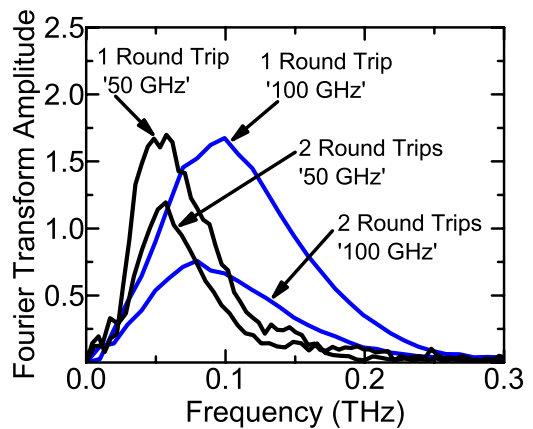


FIG. 2. (Color online) Fourier transforms of ΔR at 50 K for two samples. The “100 GHz” plots signals from a 10 nm film sample and the “50 GHz” plots represent the signals from a 20 nm film sample. The data have been rescaled so that the magnitudes of the first round trips are the same.

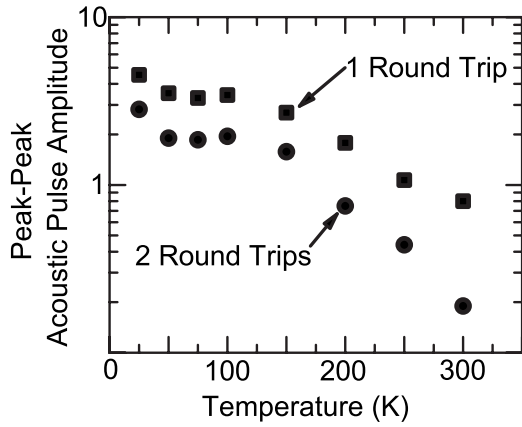


FIG. 3. Peak-to-peak amplitudes of the first (■) and second (●) ΔR pulses for the 20 nm Al-film (50 GHz) sample.

between 300 and 100 K.^{10,22} Lastly, we note that the absence of any long ringing after the initial pulses in Fig. 1 indicates that multiple reflections within the Al film were minimal in these experiments. This speaks to the good acoustic match between Si and Al and a well-bonded interface.

Figure 2 shows Fourier-transform amplitudes for the first and second pulses at 50 K for two samples: one coated with a 20 nm Al film that produced a phonon pulse with a peak at 50 GHz, and one coated with a 10 nm Al film that produced a pulse with a peak at 100 GHz. The Al-film thicknesses were determined from picosecond ultrasonic signals at short delay times (<50 ps).²¹ Rather than treating the attenuation of each Fourier component separately,^{10,11} we have chosen to identify the peak frequencies of the phonon pulses generated in each sample as the frequency measured for each case. Such an analysis could contain some error given that there is some slight frequency dependence of attenuation demonstrated in Fig. 2, but the superior signal to noise at the peak frequency gives us higher confidence in our more approximate choice of the measured frequency.

We obtain a measurement of the attenuation α of 50 and 100 GHz phonons by analyzing the changes in the peak-to-peak amplitudes of the $\Delta R(t)$ pulses from the samples.

$$\alpha = \frac{1}{d} \ln \left(\frac{|\Delta R_1|}{|\Delta R_2|} \right), \quad (2)$$

where d is the round trip distance through the Si wafer and the peak-to-peak amplitudes of the pulses detected after one and two round trips in the Si wafer are given by ΔR_1 and ΔR_2 . This simple analysis ignores any possible extrinsic losses such as those due to surface scattering. To account for these effects, we measured the samples down to $T \leq 50$ K and obtained results such as those illustrated by in Fig. 3 for the 20 nm film sample (peak frequency ~ 50 GHz) in the temperature range $25 < T < 300$ K. The attenuation obeys a $T^{2.5}$ dependence between 200 and 300 K but we find that this dependence levels off below 100 K. The low-temperature limit of the data is therefore assumed to be a measurement of acoustic attenuation that is not intrinsic to Si and represents a sum of acoustic losses at the Al/Si interface and the Si/vacuum interface at the backside of the sample. We have also

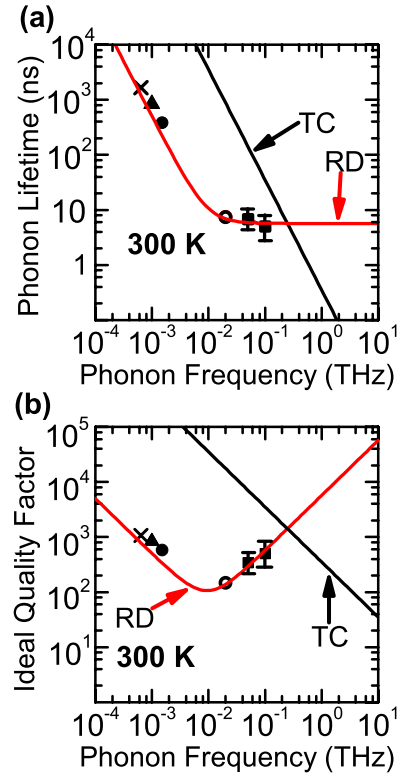


FIG. 4. (Color online) (a) Phonon lifetime versus frequency in Si at 300 K. The (■) represents our measured values of the lifetime of 50 and 100 GHz longitudinal acoustic phonons. Uncertainty was estimated by an analysis of two samples with peak frequency ≈ 50 GHz. The (○), (×), (●), and (▲) represent Refs. 11 and 23–25, respectively. Data from Ref. 24 is for [111] Si. The line labeled TC represents $\tau_{AC} = (B\omega^2 T)^{-1}$ with $B = 2.4 \times 10^{-19}$ s K⁻¹. The line labeled RD represents τ_{AC} based on α calculated using Eq. (1) with $\tau = 17$ ps. (b) Ideal quality factor $Q = f\tau$ for a nanomechanical resonator based on the data shown in part (a).

made the assumption that the optical sensitivity of the Al transducer remains independent of T . Therefore, when we apply Eq. (2) to determine the attenuation per centimeter in the silicon wafer, there is an offset that is independent of temperature that is equivalent to 51 cm^{-1} for the 20 nm film sample. We then use the data of Fig. 3 and Eq. (2) to find that the attenuation of the 50 GHz phonons in the 20 nm film sample is 138 cm^{-1} at 300 K. Thus, the intrinsic component of α for Si [100] is measured to be $138 \text{ cm}^{-1} - 51 \text{ cm}^{-1} = 87 \text{ cm}^{-1}$ at 300 K. Similar analysis of the 10 nm film sample that produced 100 GHz pulses yields an attenuation of 119 cm^{-1} at 300 K, a 37% increase over the attenuation of the 50 GHz pulses.

An important result of this work is the determination of the lifetimes of long-wavelength acoustic phonons. From $\tau_{ACoustic} = (2\alpha s)^{-1}$ we find a lifetime of 6.8 ns for 50 GHz longitudinal acoustic phonons and a lifetime of 5.0 ns for 100 GHz longitudinal acoustic phonons at room temperature. These values are significantly shorter than the value obtained by extrapolating the lifetimes of higher frequency phonons obtained from thermal conductivity data. In Fig. 4(a), we plot our measured values for the phonon lifetimes versus frequency at 300 K alongside lines representing two calcula-

tions of phonon lifetime and lifetimes determined from previous attenuation measurements.^{11,23–25} The line labeled TC in Fig. 4(a) is the function $\tau_{ACOUSTIC}=(B\omega^2T)^{-1}$ where the coefficient $B=2.4\times 10^{-19}$ s K⁻¹ has different values for normal processes ($B=2.4\times 10^{-19}$ s K⁻¹) and umklapp processes ($B=0.8\times 10^{-19}$ s K⁻¹).²⁶ If one considers the ultrasonic decay process to be an anharmonic three-phonon process, where one phonon is a very low-energy acoustic phonon, then normal processes should play the dominant role. Choosing the value for the normal processes (the higher of the two scattering coefficients), we find a function that overestimates the lifetime by a factor of 20 for 50 GHz and a factor of 8 for 100 GHz phonons. While precise agreement with experiment should not be expected from an extrapolation extending from a few THz down to 0.05 THz, the magnitude of this disagreement is significant.

A relaxation damping calculation in which α is given by Eq. (1) is in much better agreement with our 300 K data and previously published results near 1 GHz, see Fig. 4(a). To calculate the relaxation damping we make several assumptions. We have assumed that since the Gruneisen parameter for Si varies with mode and frequency from slightly less than -1 to slightly more than $+1$, we can therefore treat the RMS variation factor in the parenthesis in Eq. (1) as simply equal to 1. While this approximation would fail at low temperatures where only zone-center modes with similar values of γ are excited, it is reasonable in the temperature range studied here given that the vast majority of acoustic modes are excited at 300 K (roughly one half of the Debye temperature of Si). We used literature values for C , ρ , and s . We used a value for the thermal phonon lifetime $\tau=17$ ps, which provided the best fit to the 50 and 100 GHz data points. This value for the thermal phonon lifetime seems quite reasonable given the expected range of 30 ps (for acoustic phonons) down to 2 ps (for optical phonons).

This discrepancy between our measurements of phonon decay and predictions of acoustic-phonon lifetimes based on analysis of thermal conductivity data could play a significant role in a number of areas. One example is the enhancement of thermoelectric devices due to the “phonon drag” effect.²⁷ In such devices the relative magnitudes of the phonon lifetimes due to phonon-phonon interactions and phonon-

electron scattering directly impacts the thermopower. As was mentioned in the introduction, modeling of thermal transport in nanostructures and nanostructured materials² requires a thorough understanding of the distribution of phonon mean free paths. A third, and recently expanding area of work is in high Q , high-frequency nanomechanical resonators. While surface losses are thought to play a dominant role in the damping of high-frequency modes in nanometer scale electromechanical systems,⁷ our results indicate that intrinsic losses will contribute significantly as higher frequency resonators are investigated. Figure 4(b) is a second view of the results shown in Fig. 4(a) which plots the ideal quality factor versus frequency for a longitudinal resonator made from Si. The region of weak frequency dependence of acoustic-phonon lifetime that is indicated by our measurements implies that there is a minimum in the ideal Q factor as a function of frequency where $\omega\tau\approx 1$. Beyond this minimum there should then be a small region in the sub-terahertz range where the ideal Q factor would increase, until the point where three-phonon processes take over and the lifetime decreases as ω^2 .

In summary, we have used picosecond ultrasonics to measure the attenuation of longitudinal acoustic phonons in Si at 50 and 100 GHz. The lifetime of these phonons is measured to be roughly an order of magnitude lower than is predicted from thermal conductivity measurements. The attenuation varies with frequency and temperature in a manner that is consistent with relaxation damping. Our results indicate that intrinsic relaxational loss mechanisms will play a role in the Q factor of nanomechanical resonators in the GHz regime.

This work was partially supported by NSF under Award No. 0605000 entitled “RUI: Ultrafast Optical Studies of Nanoscale Acoustic and Thermal Transport” and also by the U.S. Department of Energy, Division of Materials Sciences under Award No. DE-FG02-07ER46459, through the Frederick Seitz Materials Research Laboratory (FSMRL) at the University of Illinois at Urbana-Champaign. The work was carried out in part in the FSMRL Central Facilities, which are partially supported by the U.S. Department of Energy under Grants No. DE-FG02-07ER46453 and No. DE-FG02-07ER46471.

¹D. G. Cahill, Wayne K. Ford, Kenneth E. Goodson, Gerald D. Mahan, Arun Majumdar, Humphrey J. Maris, Roberto Merlin, and Simon R. Phillpot, *J. Appl. Phys.* **93**, 793 (2003).

²A. S. Henry and G. Chen, *J. Comput. Theor. Nanosci.* **5**, 141 (2008).

³D. A. Broido, M. Malorny, G. Birner, N. Mingo, and D. A. Stewart, *Appl. Phys. Lett.* **91**, 231922 (2007).

⁴B. C. Daly, N. C. R. Holme, T. Buma, C. Branciard, T. B. Norris, D. M. Tennant, J. A. Taylor, J. E. Bower, and S. Pau, *Appl. Phys. Lett.* **84**, 5180 (2004).

⁵S. Ramanathan and D. G. Cahill, *J. Mater. Res.* **21**, 1204 (2006).

⁶R. Lifshitz and M. L. Roukes, *Phys. Rev. B* **61**, 5600 (2000).

⁷K. L. Ekinci and M. L. Roukes, *Rev. Sci. Instrum.* **76**, 061101

(2005).

⁸F. Hudert *et al.*, *Phys. Rev. B* **79**, 201307(R) (2009).

⁹G. Rozas, M. F. Pascual Winter, B. Jusserand, A. Fainstein, B. Perrin, E. Semanova, and A. Lemaître, *Phys. Rev. Lett.* **102**, 015502 (2009).

¹⁰H. Y. Hao and H. J. Maris, *Phys. Rev. B* **63**, 224301 (2001).

¹¹J.-Y. Duquesne and B. Perrin, *Phys. Rev. B* **68**, 134205 (2003).

¹²H. J. Maris, in *Physical Acoustics*, edited by W. P. Mason and R. N. Thurston (Academic, New York, 1971), Vol. 8, p. 279.

¹³L. Landau and G. Rumer, *Phys. Z. Sowjetunion* **11**, 18 (1937).

¹⁴I. I. Pomeranchuk, *J. Phys. (USSR)* **4**, 259 (1941).

¹⁵A. Akhieser, *J. Phys. (USSR)* **1**, 277 (1939).

¹⁶J. J. Letcher, K. Kang, D. G. Cahill, and D. D. Dlott, *Appl. Phys.*

- Lett. **90**, 252104 (2007).
- ¹⁷C. Herring, Phys. Rev. **95**, 954 (1954).
- ¹⁸T.-M. Liu, Shih-Ze Sun, Chieh-Feng Chang, Chang-Chi Pan, Guan-Ting Chen, Jen-Inn Chyi, Vitalyi Gusev, and Chi-Kuang Sun, Appl. Phys. Lett. **90**, 041902 (2007).
- ¹⁹P. G. Klemens, in *Solid State Physics*, edited by F. Seitz and D. Turnbull (Academic, New York, 1958), Vol. 7, p. 1.
- ²⁰R. M. Costescu, M. A. Wall, and D. G. Cahill, Phys. Rev. B **67**, 054302 (2003).
- ²¹C. Thomsen, H. T. Grahn, H. J. Maris, and J. Tauc, Phys. Rev. B **34**, 4129 (1986).
- ²²H. J. McSkimin, J. Appl. Phys. **24**, 988 (1953).
- ²³K. R. Keller, J. Appl. Phys. **38**, 3777 (1967).
- ²⁴A. A. Bulgakov, V. V. Tarakanov, and A. N. Chernets, Sov. Phys. Solid State **15**, 1280 (1973).
- ²⁵Y. V. Ilisavski and V. M. Sternin, Sov. Phys. Solid State **27**, 236 (1985).
- ²⁶D. G. Cahill, F. Watanabe, A. Rockett, and C. B. Vining, Phys. Rev. B **71**, 235202 (2005).
- ²⁷P. G. Klemens, *Proceedings of the Fifteenth International Conference on Thermoelectrics* (IEEE, Piscataway, NJ, 1996), p. 206.